Linking Topographical Ring Features to Geochemical and Geophysical Anomalies

Konstantin von Gunten, Stewart M. Hamilton, Zach A. DiLoreto, Md Samrat Alam, Katherine N. Snihur, Maria Dittrich, Kurt O. Konhauser & Daniel S. Alessi

View supplementary material ☑

Published online: 31 Jan 2024.

Submit your article to this journal ☑

Article views: 65

View related articles ☑

View Crossmark data ☑

Taylor & Francis
Taylor & Francis Group

Check for updates

Linking Topographical Ring Features to Geochemical and Geophysical Anomalies

Konstantin von Gunten[a], Stewart M. Hamilton[b], Zach A. DiLoreto[c], Md Samrat Alam[c], Katherine N. Snihur[a], Maria Dittrich[c], Kurt O. Konhauser[a], and Daniel S. Alessi[a]

[a]Department of Earth and Atmospheric Sciences, University of Alberta, Edmonton, Alberta, Canada; [b]Ministry of Northern Development and Mines, Sudbury, Ontario, Canada; [c]Department of Physical & Environmental Sciences, University of Toronto Scarborough, Toronto, Ontario, Canada

ABSTRACT

Circular features in forests seen from air have been studied for several decades at different locations around the world. Forest rings, as they are called in Canada's boreal forests, express several geochemical (pH, carbonate content) and geophysical (surface potential) anomalies on their 20–30 m wide ring edges. Although it has been proposed that microbial processes may cause these anomalies, the exact mechanisms of ring formation are still unknown. We focused on the Thorn North forest ring in Ontario, Canada to correlate the surface potential anomaly to soil gas concentrations. Field measurements showed that the surface potential drop at the ring edge center is framed by peaks in CO_2 production, which is linked to O_2 depletion and methane generation. Carbon isotope signatures were found to drop to lighter values (down to −20‰), suggesting increased respiration. Higher concentrations of uronic acids bound to extracellular polymeric substances were found, indicating that the surface potential anomaly is linked to respiration. 16S rRNA gene sequencing of shallow soil did not indicate a dominant microbial group on the edges; instead, principal component analysis showed that the microbial composition was controlled by the substrate (clayey vs. sandy soil), therefore future studies should focus on deeper ground layers.

Introduction

Forest rings are circular features with diameters up to 2 km that are found in the boreal forests of three provinces in Canada, namely, Manitoba, Ontario, and Québec (Mollard 1980; Veillette and Giroux 1999). Forest rings in Ontario have received considerable attention and have been characterized using geophysical, geochemical (Brauneder et al. 2016; Hamilton et al. 2004; Hamilton and Hattori 2008), and microbiological (von Gunten et al. 2018b) techniques. These Forest rings show similarities to large oval features in Western Russia (Larin et al. 2015) and Eastern US (Zgonnik et al. 2015), which are associated with hydrogen seeps from bedrock. A recent study by Malvoisin and Brunet (2023) suggested that many ground depressions around the world, including the forest rings in Canada, may be liked to geochemical reactions and hydrogen production accompanying nearby gold deposits. Such depressions might also include "fairy circles" in the Namib Desert (Getzin and Yizhaq 2019; Juergens 2013) and in Australia (Getzin et al. 2016). Other circular features that show visible similarities to forest rings are basaltic rings (flood-eroded phreatic-volcanic structures) in Washington state (US), and even similarly shaped rings on Mars (Jaeger et al. 2005). Ontario forest rings also share some similarities to so-called "fairy rings" caused by fungal mycelia (Wollaston 1807), such as lower soil pH and elevated electrical conductivity at ring edges compared to the surroundings (Bonanomi et al. 2012). However, to date, no links between fungal infestation of trees to the vegetation patterns in forest rings have been identified. Furthermore, a lack of measurable growth in diameter and the presence of a physical dip in the mineral soil at the ring edge have been observed (Giroux 1998; Hamilton et al. 2004; Veillette and Giroux 1999; Veillette and Smith 1992).

Canada's forest rings are characteristically located over carbonate-rich deposits and have more reducing soil conditions in the center of the ring, which are associated with the presence of methane or hydrogen sulfide (Hamilton and Hattori 2008). The physical dip on the edges was previously proposed to be caused by increased acidity and resulting carbonate dissolution (Hamilton et al. 2004). Typical for the forest rings was a negative spike in soil electrical surface potential or self-potential (SP) at the ring edges. SP should not be mistaken with the oxidation-reduction-potential (ORP). While SP and ORP can influence each other (Naudet and Revil 2005) they are not directly linked, and their values can vary independently. The measurement of self-potential is a geophysical method used for mineral exploration by detecting current flows through ore bodies

and surrounding groundwater (Sheriff 2022). Suppressed tree growth, thicker peat covers, wetter conditions (Veillette and Giroux 1999) and strong redox gradients were reported at the forest ring edges (Hamilton and Hattori 2008). Collectively, these observations led to the hypothesis that microbial processes might be involved in the expression of these ring structures (Hamilton and Hattori 2008). Supporting this hypothesis, an increased abundance of *Geobacter* species was observed at the ring edge of the so-called "Bean" and "Thorn North" rings in Ontario (von Gunten et al. 2018b). However, it was unclear if the physio-chemical gradients at the ring edges were governed by biological processes and how they might be related to the physical dip in the mineral soil.

Building on the findings by von Gunten et al. (2018b) we attempted here to test the hypothesis that the geophysical SP-anomaly of the forest rings is linked to processes associated with microbial activities. We investigated the so-called "Thorn North" ring (Figure 1), a 560 m wide ring located near Timmins, Ontario, Canada in more detail. Here, along with denser SP probing compared to the 2018 study, we monitored soil gases (O_2, CO_2, and CH_4), applied analysis of stable isotopes of carbon, 16S rRNA gene sequencing, and EPS compositions at two transects within Thorn North ring.

Materials and methods

Field site

The research area is located in the boreal shield climate zone and is part of the Abitibi plains eco-region of Canada. The region experiences an annual average precipitation of 835 mm and daily average temperatures from $-17\,°C$ to $+16\,°C$ (Timmins station 1981–2010 from http://climate.weather.gc.ca/climate_normals/). Glacial retreat in this region about 9400 years ago deposited quaternary sediments, most prominently clay-rich glacial lake sediments (Dyke 2004). Around 8400 years ago the glaciers advanced back into the region during which sand- and clay-rich Cochrane till was deposited on top. The glaciers eventually receded, and the glacial lakes drained 7600 years ago, allowing peat to form in the area. The bedrock in this area consists of a quartz-feldspar porphyry with minor sulfide content starting at about 30 m depth (Hamilton and Hattori 2008). Two different transects were chosen for the investigation based on differences in the soil cover (peat vs. humus; sand vs. clay), humidity, and geochemical gradients, which were previously reported by Brauneder et al. (2016).

In-situ field measurements

Field investigations in August 2018 focused on the East (E) ring edge ("clay line," Figure 1) and on the Southwest-Northeast (SW-NE) transect ("sand line") and are described in detail in the open file report by von Gunten et al. (2018a). The sampling was planned to fully cover the laterally narrow (5–10 m) ring edges. Easier access to the E
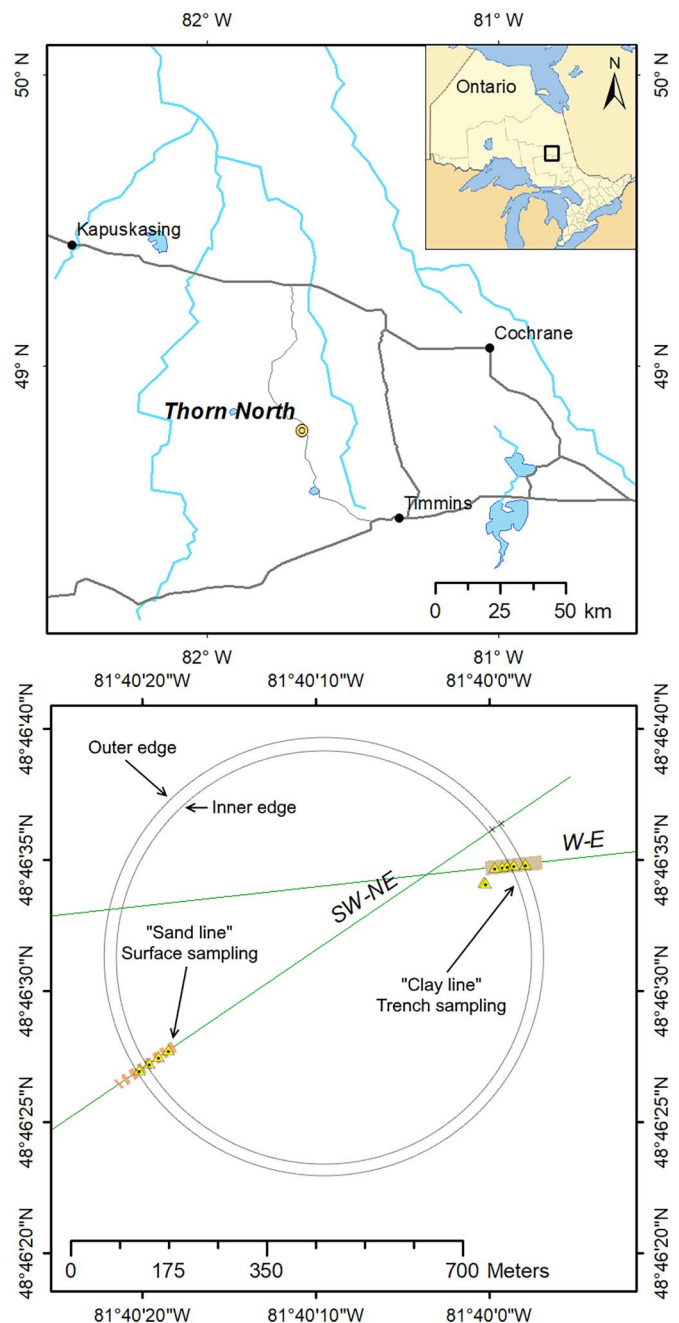
Figure 1. Location of the Thorn North ring as well as the two sampled transects: E-transect "clay line" and the SW-transect "sand line."

transect allowed the use of a backhoe to create a 60 cm wide and 1.5 m deep trench, to get a better picture of the soil profiles along the forest ring boundary.

Measuring SP is a passive method to detect spontaneous or natural electrical potential due to electrochemical interactions between fluids and minerals, electrokinetic processes from the flow of groundwater, or thermoelectric mechanisms due to temperature gradients (Corwin and Hoover 1979). Larger potentials are, for example, generated if more conductive mineralized materials are available. A Consort C864 multi-channel BNC data logger was used to record the SP at each site. The electrical apparatus included 2 platinum lances and an Ag–AgCl reference electrode, by which voltage

was measured using the data logger against a second, stationary Ag–AgCl reference electrode at a base station located 50 m outside the ring edge for SP measurements. Before every deployment, the mobile platinum lance was soaked for 30 sec in a reducing pretreatment solution (acidic ferrous sulfate; Hanna Instruments HI7091L) designed to facilitate faster response times for metallic electrodes. Both sampling electrodes and the base station electrode were connected to the data logger using an approximately 200 m-long reel of two-strand shielded electronic wire. The shielding was grounded 1 m away from the base station against a metal spike. The electrodes at the E transect were placed 2 cm below the sand surface resulting in depths of 34–90 cm below ground surface due to variable sand layer thickness. The procedures were similar on the SW-NE transect; however, due to the lack of a trench, the electrodes were emplaced vertically into the soil. On both transects, 1-cm diameter holes were drilled 5 cm deep into soil – horizontally on the E line and vertically on the SW-NE transect. To make an electrical connection with the soil and to avoid damaging the glass reference electrodes, presoaked, gelled bentonite was extruded into the 1-cm holes and the glass reference electrode was inserted, similar to Timm and Möller (2001). To cover the entire transect, the base station was moved every 140–250 m.

At the E edge, soil temperature was recorded at the SP measuring location using a soil thermometer pushed into the shaded trench side. 15 mL of soil samples were taken and mixed in the field with 30 mL of distilled water. Once homogenized, pH and conductivity of the slurry was determined with the data logger. These data are not specifically discussed here; however, they are shown in Figure S1.

Gas collection and analysis

Gas samples were collected using a 1.5 m long steel tube, equipped with a slide hammer (Lovell et al. 1983). The tube was hammered down to 30–50 cm (avoiding soil water), and gas was withdrawn, using a hand pump, into 500–1000 L Tedlar bags. The gas was measured for O_2, CO_2 and CH_4 content in the field using an RKI Eagle multi-gas meter (Model 71-0028RK) equipped with an infrared CO_2 sensor, an electrochemical oxygen sensor and two methane sensors. The field testing consumed about half the gas in the Tedlar bags, and the other half was used for the analysis of δ^{13}C-CO_2 at the Ján Veizer Stable Isotope Laboratory at the University of Ottawa. The analysis was carried out using a Thermo-Fisher GC-Isolink gas chromatograph and a Delta V isotope ratio mass spectrometer.

Sample collection

Soil sampling for chemical and biological analyses at the E edge (clayey soil) was performed along the south wall of the trench 2 cm below the sand layer, similar to the SP measurement. Here, the soil was extracted using a sterilized soil spoon. After discarding the outermost 2 cm of the sample, the rest was packed into separate polypropylene tubes for 16S rRNA gene sequencing (for characterization of bacteria/archaea), EPS extraction, and chemical analyses. At the SW ring edge (Figure 1), samples were extracted from 40 cm depth at selected locations based on the surface potential in situ measurements. The sandy sample was retrieved with a hand auger and distributed with a sterile spatula into corresponding sample containers, as described above. Samples were transported using dry ice and kept at −20 °C until further processing.

Microbiological methods

16S rRNA gene sequencing

DNA was extracted from soils, peat, and selected sporocarp samples using the RNeasy PowerSoil Kit (Qiagen) using a method similar to Fredricks et al. (2005). If required, the extracted DNA was concentrated up to 2 ng/µL using ethanol precipitation (sodium acetate buffer, pH 5.5) as described by MRC-Holland (2008), a method based on Zeugin and Hartley (1985) and final concentrations were verified using a Qubit Fluorometer (Thermo Fisher). The samples were sent out for 16S rRNA gene sequencing and pipeline processing to the MR DNA laboratory (Shallowater, TX, USA) using the Illumina MiSeq targeting the V4 variable region (forward primer F515 GTGYCAGCMGCC GCGGTAA, reverse primer R806 GGACTACNVGGGTW TCTAAT). Operational taxonomic units (OTUs) were defined by clustering at a 97% similarity level and taxonomically classified using BLASTn (Altschul et al. 1990). Data interpretation was performed using METAGENassist (Arndt et al. 2012) and R (v. 3.5.2) with the PHYLOSEQ package (McMurdie and Holmes 2013).

Extracellular polymeric substances extraction and composition analysis

EPS from soil was extracted using the cation exchange resin (CER) method (Frølund et al. 1996; Redmile-Gordon et al. 2014) with the DOWEX Marathon C resin (Supplementary Information). Briefly, 1 g of soil was mixed with 3–8 g resin (depending on the amount of carbon) and 25 mL of phosphate buffer. After 2 h, the mixtures were centrifuged (4000 g, 30 min) and the supernatant combined with 70% ethanol. After 8 h of precipitation at 4 °C, an EPS pellet was recovered by centrifugation as described above, which was then purified via dialysis (14 kDa) for 12 h. Concentrations of carbohydrates, proteins, and uronic acids of EPS were determined using colorimetric methods measured on a microplate reader (Molecular Devices, USA). Carbohydrates were measured using the phenol-sulfuric acid method (Dubois et al. 1956; Klock et al. 2007; Redmile-Gordon et al. 2014; Underwood et al. 1995). Proteins were measured using the Bradford assay (Bradford 1976; Klock et al. 2007). Uronic acids were determined using galacturonic acid equivalents (Blumenkrantz and Asboe-Hansen 1973; Klock et al. 2007).

Data analysis

Data series were correlated using the Pearson's correlation coefficient. Principal component analysis was done using Origin Pro version 8.6.

Results and discussion

General surface characteristics

The transects varied strongly in terms of soil layering and soil properties. The peat thickness at the E edge was on average $36 \pm 12\,cm$ ($n = 21$), with a thicker peat layer outside the ring ($45 \pm 10\,cm$) than inside ($28 \pm 10\,cm$) (Figure S1). The organic layer (mostly dry humus) was patchy at the SW-NE line and nearly absent at the sampling locations. Here, a thin humus layer of 2–3 cm was present with the sand directly below it. The moisture content in the mineral soil samples was on average higher in the clay ($20 \pm 5\%$) than the sand ($13 \pm 4\%$), with highest numbers being reached at the ring edge for both transects (Figure S2).

Changes in SP and gas composition

The SP survey revealed a drop in potential at the ring edges of both transects. The drop was approximately 30 mV (down to −14 mV) at the sand line SW edge and 50 mV (down to −21 mV) at the sand line NE edge (Figure 2). The effect was stronger at the clay line E edge at 75 mV (down to −89 mV). SP is a relative voltage measurement, dependent on the placement of the stationary electrode and therefore it is the discrete, high contrast nature of these responses and their coincidence with the ring edge that are significant, rather than their absolute magnitude. However, for context, these SP ranges are typical of responses in soils over sulfide ore deposits (eg, Rani et al. 2020). Repeat SP measurement in 2019 on the NE ring edge (Hamilton et al. 2019) produce responses that were very similar, demonstrating that the SP signal has temporal stability.

The SP drops are coincident with O_2 depletion (expressed as air O_2 concentration minus measured value) and increased concentrations of CO_2. O_2 was also found to be depleted near the inside of the E edge at 340 m. At the SW edge of the sand line and the E edge, spikes in CO_2 were accompanied by increased CH_4 concentrations (370 ppm and 1500 ppm, respectively). The maximum anomaly for the SP values is framed by O_2 minima and concentration peaks for CO_2 and CH_4. These shifted positions of the peaks lead to a low Pearson's correlation between these parameters (between −0.10 to 0.00, Table S3). A positive Pearson's correlation coefficient was found between the gas components; for CH_4 and CO_2 concentrations (0.48) as well as for CO_2 concentrations and O_2 depletion (0.88), indicating that the gas composition is related to respiration/fermentation processes. Anomalous O_2 depletions and CH_4 enrichments of varying contrast were also previously noted at Thorn North in the headspace of monitoring wells at six out of six ring edge transects (Hamilton and Hattori 2008). CO_2 was not measured in that study.

The isotopic signature was near the typical range of soil respired CO_2 (usually <-15‰), which depends on the composition of the organic matter (Cerling et al. 1991; Graven et al. 2020) and would also be affected by atmospheric diffusion of CO_2 into the forest soil (Bowling et al. 2015). The influence of diffusion becomes apparent when considering that the $\delta^{13}C$ were relatively similar in both transects (SW-NW vs. E) despite having different soil composition (sand vs. clay), in which the expected permeability would clearly be different. Repeat $\delta^{13}C$ measurements for two samples collected side-by-side at a ring edge (data not shown) had a variation in concentration (difference of 0.28 vol.%) and $\delta^{13}C$ values (difference of 4.63‰), indicating an uneven or patchy distribution of CO_2-producing zones. Despite the variations, clear patterns along the ring edges could be found. For instance, a lighter isotopic composition of the CO_2 was found for the edge samples, reaching −18.42‰, −20.08‰, and −16.45‰ for the SW, NE, and E edges, respectively. This suggests increased respiration on the ring edges that would drive the $\delta^{13}C$ toward lighter values (Unger et al. 2010). The correlation between the field parameters can be shown in the form of a principal component analysis (Figure 3). The distribution of sampling points and parameters indicate the x-axis (PC1) primarily determines if the sample comes from the SW-NE or the E sector. The distribution of the parameter vectors suggests that the two ring transects vary in soil moisture, and contents of N, organic matter, and carbonates, which can be expected due to the differing soil properties. The y-axis (PC2), on the other hand, separates the edge vs. non-edge samples. PC2 is also strongly determined by SP and gas-related parameters, suggesting that ring edge samples are strongly affected by changes in these parameters. With our data we can therefore link the large topographic features of forest rings to geophysical (SP) and geochemical (gas concentrations and C isotopes) surface expressions.

Microbial composition and EPS characteristics

High variability of prokaryotic communities was observed in both ring edges (Figure S3). The communities in samples from a given transect were more similar to each other than to samples from another transect, but from a similar relative location (eg, inside ring, outside ring, ring edge). This was confirmed by PCA (Figure S4). The communities at the E edge (clay line) were characterized by a high abundance of Deltaproteobacteria (up to 34%) and Anaerolineae (up to 23%), mainly contributed by OTUs similar to the genera *Pelobacter*, *Geobacter*, *Bellilinea*, *Levilinea*, and *Anaerolinea*. At the E ring edge itself, a notably high abundance of the classes Gemmatimonadetes (7%), Methanomicrobia (2%), Negativicutes (4%), and Chloroflexia (7%) was found (Table S1). The communities at the SW edge were characterized by a high abundance of Holophagae (up to 31%) and Alphaproteobacteria (up to 23%), mainly due to bacteria like *Holophaga*, *Rhodoplanes* and *Stella* (Table S2). At the location with the lowest SP values of the SW edge, there was a notably high abundance of the classes Bacteroidetes (3%) and Thaumarchaeota (3%). These differences
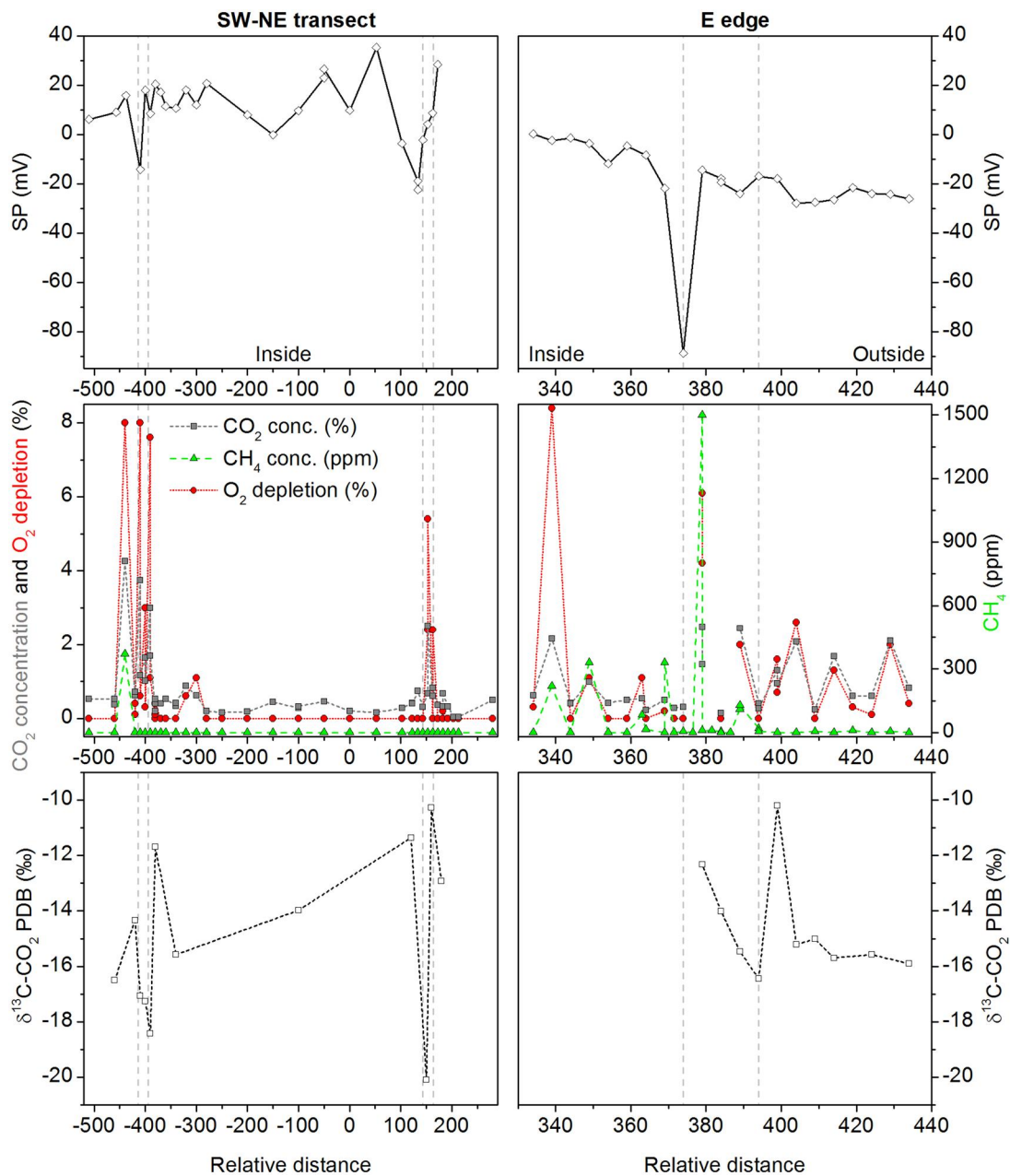
Figure 2. Surface potential in-situ measurements, gas concentrations, O_2 depletion expressed as a positive response ($[O_2]_{air}$-$[O_2]_{measured}$), and $\delta^{13}C$ of CO_2 in soil gas at the SW-NE transect and the E edge. The dashed lines indicate the position of the ring edges.

can be explained by the amount of soil clay content, which can have an even greater effect on microbial composition and diversity than carbon sources (Olagoke et al. 2022). This effect makes comparison between ring edges or even different rings difficult, and these challenges should be considered in future studies.

The SP response correlated in a positive way (0.46 and 0.41) to species richness (Chao1) and diversity (Inv. Simpson), respectively, indicating that the highest species richness would be found outside the SP lows on the ring edge, ie, in the zones framing the SP anomaly. This corresponds to previous observations by von Gunten et al. (2018b) that the lowest diversity is found within the ring edge, while the boundaries of the edge show a high diversity.

Extracted and purified EPS from the SW and E edges had high abundances of uronic acids close or at the ring

edges (Figure 4). Uronic acids concentrations spiked to as high as 1.3 mg/g at the SW edge. The increase in uronic acids was more than 5x higher at the E edge, reaching 7.4 mg/g. This is likely because clay provides a better matrix for EPS production due to increased aggregate stability (Olagoke et al. 2022). The standard deviation of the EPS results was small, indicating that the peaks were not random due to local accumulation of organic matter. SP correlated in a negative way to concentrations of carbohydrates and uronic acids (−0.54 and −0.41, respectively, Table S3), suggesting that at the SP lows, high concentrations of these molecules were present. Note that similar to the EPS, a stronger change in SP was found in the clay.

With our data we cannot conclusively link microbiological activity with the observed SP- and soil gas-anomalies in a forest ring. However, elevated EPS concentrations,
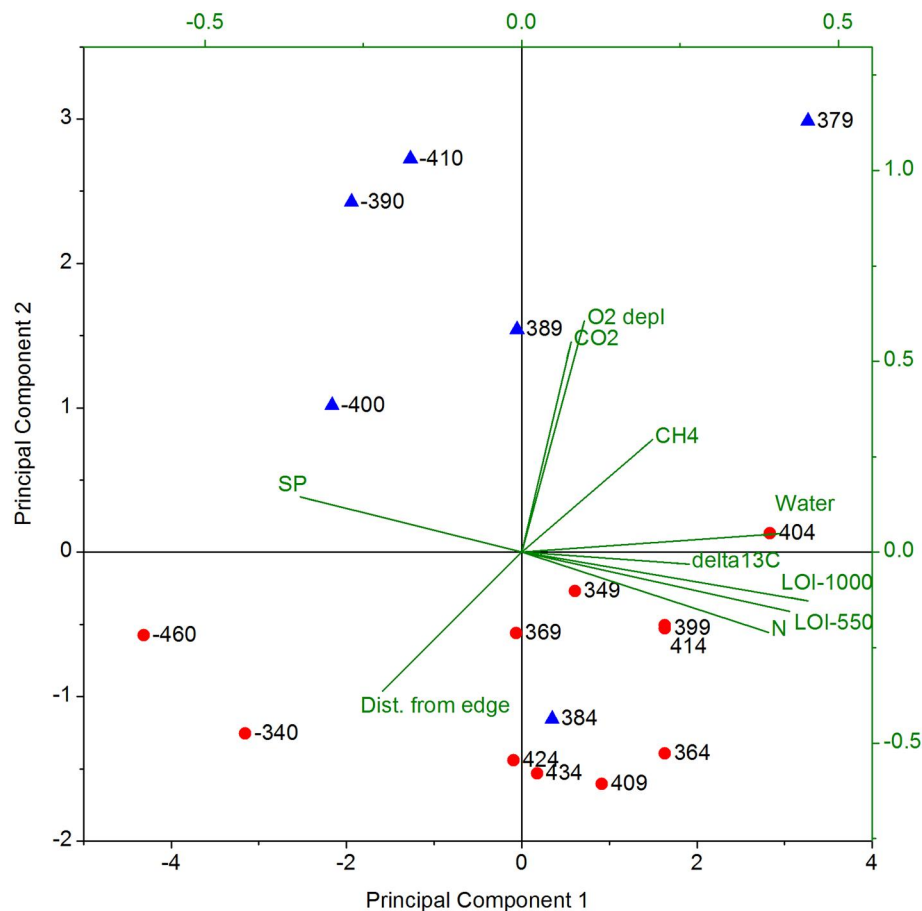
Figure 3. Principal component analysis for data on SP, soil gas concentrations, isotopic composition, LOIs, N and water contents. Data points labeled with the point coordinates relative to a common reference. Negative values represent SW transect values, positive values represent the E transect. Ring edge points marked with blue triangles. The PCA was based on the correlation matrix with 5 extracted components. Note that the axes scales are different for data points (left and bottom axes) and variables (right and top axes) for better visibility. Percentages of variance for PC1 and PC2 were 41.7% and 24.2%, respectively.

increased O_2 consumption and lighter $\delta^{13}C$ signatures lead us to propose stronger microbial activity in the anomaly zones. Williams et al. (2007) showed that SP signals can be associated with increased microbial sulfate reduction. Naudet and Revil (2005) showed a link between SP and microbial-induced ORP changes suggesting the linear correlation: $SP = 0.2 \cdot E_H - E_H^0$). Although their experimental conditions were different, we estimate a bacterial-induced redox potential difference of $-88\,mV$ and $-445\,mV$ for the sand and clay lines, respectively. These values lie in the range of reductive metabolisms, such as methanogenesis, iron and sulfate reduction.

Conclusions

The ring edges (up to 30 m wide) of the Thorn North ring are zones of strong gradients in various parameters, especially geochemistry. The drop in SP is framed toward outside and inside of the ring by peaks in CO_2 and/or CH_4 production and O_2 consumption. At the ring edges, increased concentrations of carbohydrates and uronic acids in microbial EPS were shown, which suggests stronger bacterial growth in the gradient zones. In addition, the stable carbon isotopic composition ($\delta^{13}C$) of CO_2 suggested increased organic matter degradation (and thus increased

respiration). EPS concentrations and the strength of the SP anomaly were strongly affected by the substrate. In the clay-rich E-edge of the ring, higher EPS concentrations and a higher contrast SP anomaly were observed. Microbial community composition was also affected by the substrate, yielding very distinct communities for the two ring transects.

A link between SP, soil gas and carbon isotopes has been shown, and these are significant discoveries. However, we cannot conclusively link the microbial composition to the conditions found at the ring edges. Differences in substrate (sand vs. clay) made it difficult to find clear differences in the microbial communities at the ring edges, where the highest SP- and gas-anomalies were observed. Future studies should take this into account. One way to control the substrate differences could be by taking deeper samples which originate from the same soil layers. The acquisition of deeper soil gas from the mineral soil layers should be attempted and systematically collected over the complete transects through one or more forest rings. One such attempt is described in the open file report by Hamilton et al. (2019).

Further research on microorganisms should focus on their activity, for example using RNA analysis and/or phospholipid fatty acid (PFLA) analysis, instead of applying 16S rRNA sequencing as this method may not represent
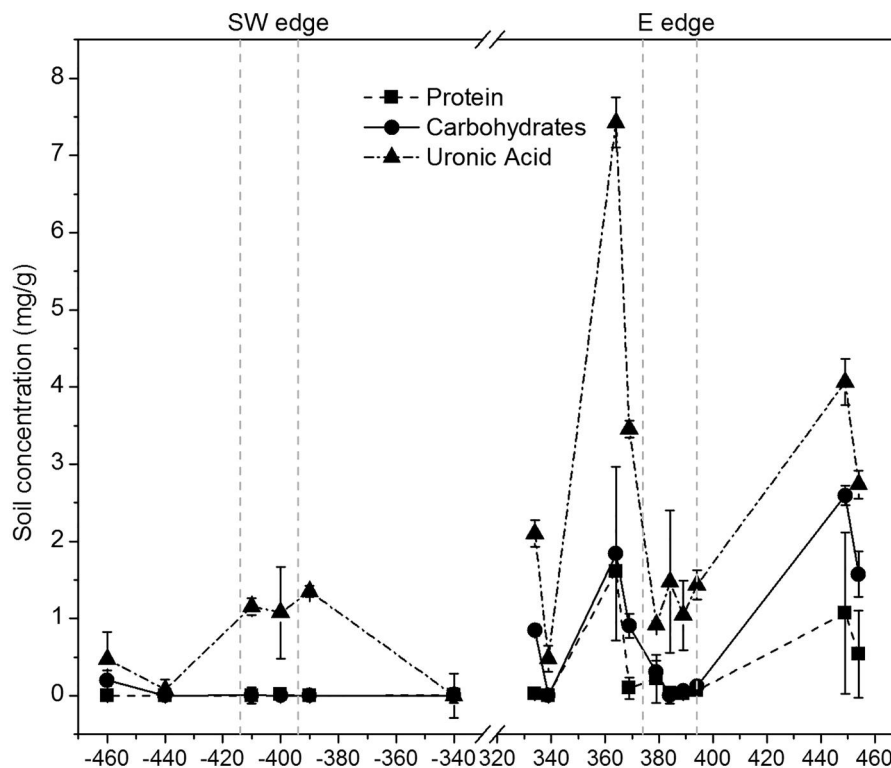
Figure 4. Extractable fractions of EPS including proteins, carbohydrates and uronic acids along the sampling transects. Values on x-axis show the relative lateral distance on the corresponding transects (in m). dotted lines represent forest ring boundaries. Error bars represent standard deviations (n = 3).

actively metabolizing groups. The research should also include other gas species that are linked to microbial or geogenic processes, such as H_2, a soil gas that has attracted increasing recent interest.

Acknowledgments

Disclosure statement

No potential conflict of interest was reported by the author(s).

Funding

References

Altschul SF, Gish W, Miller W, Myers EW, Lipman DJ. 1990. Basic local alignment search tool. J Mol Biol 215(3):403–410.

Arndt D, Xia J, Liu Y, Zhou Y, Guo AC, Cruz JA, Sinelnikov I, Budwill K, Nesbø CL, Wishart DS. 2012. METAGENassist: a comprehensive web server for comparative metagenomics. Nucleic Acids Res 40(Web Server issue):W88–W95.

Blumenkrantz N, Asboe-Hansen G. 1973. New method for quantitative determination of uronic acids. Anal Biochem 54(2):484–489.

Bonanomi G, Mingo A, Incerti G, Mazzoleni S, Allegrezza M. 2012. Fairy rings caused by a killer fungus foster plant diversity in species-rich grassland. J Veg Sci 23(2):236–248.

Bowling DR, Egan JE, Hall SJ, Risk DA. 2015. Environmental forcing does not induce diel or synoptic variation in the carbon isotope content of forest soil respiration. Biogeosciences 12(16):5143–5160.

Bradford MM. 1976. A rapid and sensitive method for the quantitation of microgram quantities of protein utilizing the principle of protein-dye binding. Anal Biochem 72(1-2):248–254.

Brauneder K, Hamilton SM, Hattori K. 2016. Geochemical processes in the formation of 'forest rings': examples of reduced chimney formation in the absence of mineral deposits. GEEA 16(1):85–99.

Cerling TE, Solomon DK, Quade JAY, Bowman JR. 1991. On the isotopic composition of carbon in soil carbon dioxide. Geochim Cosmochim Acta 55(11):3403–3405.

Corwin RF, Hoover DB. 1979. The self-potential method in geothermal exploration. Geophysics 44(2):226–245.

Dubois M, Gilles KA, Hamilton JK, Rebers PT, Smith F. 1956. Colorimetric method for determination of sugars and related substances. Anal Chem 28(3):350–356.

Dyke AS. 2004. An outline of North American deglaciation with emphasis on central and northern Canada. In: Ehlers J, Gibbard PL, editors. Developments in Quaternary Sciences. Amsterdam, Netherlands: Elsevier; Volume 2, Part B, p. 373–424.

Fredricks DN, Smith C, Meier A. 2005. Comparison of six DNA extraction methods for recovery of fungal DNA as assessed by quantitative PCR. J Clin Microbiol. 43(10):5122–5128.

Frølund B, Palmgren R, Keiding K, Nielsen, PH. 1996. Extraction of extracellular polymers from activated sludge using a cation exchange resin. Water Res 30(8):1749–1758. https://www.sciencedirect.com/science/article/abs/pii/0043135495003231

Getzin S, Yizhaq H. 2019. Unusual Namibian fairy circle patterns in heterogeneous and atypical environments. J Arid Environ 164:85–89.

Getzin S, Yizhaq H, Bell B, Erickson TE, Postle AC, Katra I, Tzuk O, Zelnik YR, Wiegand K, Wiegand T, et al. 2016. Discovery of fairy circles in Australia supports self-organization theory. Proc Natl Acad Sci U S A 113(13):3551–3556.

Giroux JF. 1998. Végétation, morphologie et dynamique de sept anneaux géants blanchâtres retrouves dans les peuplements d'épinettes noires dans le nord de l' Abitibi. M.Sc. Département des sciences biologiques. Montréal, Québec, Canada: Université du Québec à Montréal.

Graven H, Keeling RF, Rogelj J. 2020. Changes to carbon isotopes in atmospheric CO2 over the industrial era and into the future. Global Biogeochem Cycles 34(11):e2019GB006170.

Hamilton SM, Burt AK, Hattori KH, Shirota J. 2004. The distribution and source of forest ring-related methane in northeastern Ontario; in summary of field work and other activities, 2004, Ontario Geological Survey Open File Report 6145, p.21-1 to 21-26. Accessed November 2023. Available at https://www.geologyontario.mndm.gov.on.ca/index.html.

Hamilton SM, Hattori KH. 2008. Spontaneous potential and redox responses over a forest ring. Geophysics 73(3):B67–B75.

Hamilton SM, von Gunten K, Sherwood Lollar B, DiLoreto ZA, Alam MS, Snihur K, Majeed H, Alessi DS, Dittrich M, Konhauser KO, et al. 2019. Soil gas compositional changes and electrical field (SP) responses at the edges of the Thorn North forest ring; in Summary of Field Work and Other Activities, 2019, Ontario Geological Survey, Open File Report 6360, p.19-1 to 19-9. Accessed January 2023. Available at https://www.geologyontario.mndm.gov.on.ca/index.html.

Jaeger WL, Keszthelyi LP, Burr DM, Emery JP, Baker VR, McEwen AS, Miyamoto H. 2005. Basaltic ring structures as an analog for ring features in Athabasca Valles, Mars. Paper presented at: 36th Annual Lunar and Planetary Science Conference, League City, Texas, USA.

Juergens N. 2013. The biological underpinnings of Namib Desert fairy circles. Science 339(6127):1618–1621.

Klock J-H, Wieland A, Seifert R, Michaelis W. 2007. Extracellular polymeric substances (EPS) from cyanobacterial mats: characterisation and isolation method optimisation. Mar Biol 152(5):1077–1085.

Larin N, Zgonnik V, Rodina S, Deville E, Prinzhofer A, Larin VN. 2015. Natural molecular hydrogen seepage associated with surficial, rounded depressions on the European craton in Russia. Nat Resour Res 24(3):369–383.

Lovell JS, Hale M, Webb JS. 1983. Soil air carbon dioxide and oxygen measurements as a guide to concealed mineralization in semi-arid and arid regions. J Geochem Explor 19(1-3):305–317.

Malvoisin B, Brunet F. 2023. Barren ground depressions, natural H2 and orogenic gold deposits: spatial link and geochemical model. Sci Total Environ 856(Pt 1):158969.

McMurdie PJ, Holmes S. 2013. Phyloseq: an R package for reproducible interactive analysis and graphics of microbiome census data. PloS one 8(4):e61217. http://doi.org/10.1371/journal.pone.0061217

Mollard JD. 1980. Landforms and Surface Materials of Canada: A Stereoscopic Atlas and Glossary, 6th ed. Regina: Mollard.

MRC-Holland. 2008. Protocol ethanol precipitation of DNA. Accessed March 2019. Available at https://www.mlpa.com/WebForms/WebFormDBData.aspx?Tag=_wl2zCji-rCGANQgZPuTixn01pTTvc Nt -SNVkcQD5y3xpa11bK1W4GRNLbjV7Lemdz9tEz0HK5jxaciubz5YR vA.

Naudet V, Revil A. 2005. A sandbox experiment to investigate bacteria-mediated redox processes on self-potential signals. Geophys Res Lett 32(11):L11405.

Olagoke FK, Bettermann A, Nguyen PTB, Redmile-Gordon M, Babin D, Smalla K, Nesme J, Sørensen SJ, Kalbitz K, Vogel C. 2022. Importance of substrate quality and clay content on microbial extracellular polymeric substances production and aggregate stability in soils. Biol Fertil Soils 58(4):435–457.

Rani K, Guha A, Pal SK, Kumar KV. 2020. Broadband reflectance, emittance spectroscopy and self-potential geophysical survey for targeting gold sulphide lode deposit in Bhukia, Rajasthan, India. Geocarto Int 35(1):93–112.

Redmile-Gordon M, Brookes P, Evershed R, Goulding K, Hirsch P. 2014. Measuring the soil-microbial interface: extraction of extracellular polymeric substances (EPS) from soil biofilms. Soil Biol Biochem 72:163–171.

Sheriff RE. 2022. Earth exploration. Encyclopedia Britannica. Accessed January 2023. Available at https://www.britannica.com/topic/Earth-exploration.

Timm F, Möller P. 2001. The relation between electric and redox potential: evidence from laboratory and field measurements. J Geochem Explor 72(2):115–128.

Underwood G, Paterson D, Parkes R. 1995. The measurement of microbial carbohydrate exopolymers from intertidal sediments. Limnol Oceanogr 40(7):1243–1253.

Unger S, Máguas C, Pereira JS, Aires LM, David TS, Werner C. 2010. Disentangling drought-induced variation in ecosystem and soil respiration using stable carbon isotopes. Oecologia 163(4):1043–1057.

Veillette JJ, Giroux JF. 1999. The Enigmatic Rings of the James Bay lowland: A Probable Geological Origin. Natural Resources Canada, Geological Survey of Canada, Montréal, Québec, Canada.

Veillette JJ, Smith ML. 1992. Les grands anneaux du nord de l'Abitibi, un nouvel outil de datation relative? 7ieme Congres de l' Association québécoise pour l'étude du Quaternaire, Rouyn-Noranda, Québec, 23-27 septembre, 1992. Programme et Résumés, Bulletin de l' AQQUA. 18(2):76.

von Gunten K, Hamilton SM, DiLoreto ZA, Alam MS, Alessi DS, Dittrich M, Sherwood Lollar B, Konhauser KO, Dell KM. 2018a. Biogeochemical and electrical investigations in soils at the Thorn North forest ring; in Summary of Field Work and Other Activities, 2018, Ontario Geological Survey, Open File Report 6350, p.21-1 to 21-13. Accessed January 2023. Available at https://www.geologyontario.mndm.gov.on.ca/index.html.

von Gunten K, Hamilton SM, Zhong C, Nesbø C, Li J, Muehlenbachs K, Konhauser KO, Alessi DS. 2018b. Electron donor-driven bacterial and archaeal community patterns along forest ring edges in Ontario, Canada. Environ Microbiol Rep 10(6):663–672.

Williams KH, Hubbard SS, Banfield JF. 2007. Galvanic interpretation of self-potential signals associated with microbial sulfate-reduction. J Geophys Res 112(G3):G03019.

Wollaston WH. 1807. VII. On fairy-rings. Philos Trans R Soc Lond 97:133–138. http://doi.org/10.1098/rstl.1807.0008

Zeugin JA, Hartley JL. 1985. Ethanol precipitation of DNA. Focus 7(4):1–2.

Zgonnik V, Beaumont V, Deville E, Larin N, Pillot D, Farrell KM. 2015. Evidence for natural molecular hydrogen seepage associated with Carolina bays (surficial, ovoid depressions on the Atlantic Coastal Plain, Province of the USA). Prog Earth Planet Sci 2(1):31.